Full-Scale Wind Tunnel Test of a Helicopter Individual Blade Control System

Stephen A. Jacklin and Khanh Q. Nguyen
NASA Ames Research Center
Moffett Field, CA

Achim Blaas and Peter Richter
ZF Luftfahrttechnik, GmbH
Germany

Abstract

A helicopter individual blade control (IBC) system was tested on a full-scale BO 105 rotor in the NASA Ames 40- by 80-Foot Wind Tunnel. For this test, the rotating pitchlinks were replaced by servo-actuators developed by ZF Luftfahrttechnik, Germany. Using these actuators, IBC inputs consisting of single-frequency harmonics (2P to 6P), pitch pulses, pitch wavelets, and doublet pitch schedules were introduced in an open-loop manner. IBC inputs of 1P-12P were also tested without blades. An extensive amount of data were acquired for each IBC data point. These data include rotor performance, vibratory hub forces and moments, blade loads, control system loads, blade root pitch motion, blade tip accelerations, and BVI noise data. These data indicate very significant reductions of all vibratory rotor forces and moments and suppression of BVI noise using IBC.

Introduction

A wind tunnel test was conducted with a full-scale helicopter rotor to evaluate the potential of open-loop individual blade control (IBC) to improve rotor performance, to reduce blade vortex interaction (BVI) noise, and to alleviate rotor hub vibration. The wind tunnel test was an international collaborative effort between NASA/U.S. Army AFDD, ZF Luftfahrttechnik GmbH, the Deutsche Forschungsanstalt fur Luft- und Raumfahrt (DLR), and Eurocopter Deutschland GmbH (ECD). The program was conducted under the auspices of the U.S./German Memorandum of Understanding (MOU) on Rotorcraft Aeromechanics.

Individual blade control was realized by replacing the standard pitch-links with servo-actuators. These high-frequency actuators allowed the pitch of each blade to be controlled independently of each other. The specially designed servo-actuators and IBC control system were designed and manufactured by ZF Luftfahrttechnik GmbH. The wind tunnel test was conducted in the 40- by 80-Foot Wind Tunnel at the NASA Ames Research Center. The rotor system used for the test was a full-scale BO 105 rotor system mounted on the NASA/Army Rotor Test Apparatus (RTA).

Presented at the American Helicopter Society 50th Annual Forum, Washington, DC, May 11-13, 1994.

The ability to individually control the angle of attack of each rotor blade had been desired ever since the pioneering work of Kretz [Ref. 1], Lemnios [Ref. 2], McCloud [Ref. 3], and Ham [Ref. 4]. These investigators realized that helicopter control through the conventional swashplate, whether for trim or other objectives, was fundamentally limited for rotor systems with four or more blades. In that case, specification of the pitch (or servo-flap) control of one blade predetermined the control for the other blades. This shortcoming of the conventional swashplate limits the degrees of freedom available for reducing rotorcraft vibrations and acoustics because the swashplate does not permit changing the pitch of one blade without changing the pitch of the other blades at the same time. Nevertheless, owing to the expense and added complexity of IBC control systems, the related and less complex technique of higher harmonic control (HHC) using conventional swashplate actuators was explored first. Today, it is recognized that HHC has been extensively investigated through analytical methods, wind tunnel testing, and flight tests. Although these studies have shown HHC to be effective for vibration reduction and BVI noise suppression (Refs. 5-14), the weight of the hydraulic system and constraints of the swashplate geometry limit its overall effectiveness to the point where the benefit obtained using HHC approaches its cost to implement. For this reason, HHC systems have not seen usage in very many commercial applications.

The first set of high-bandwidth actuators developed for the rotating system were designed by ZF Luftfahrttechnik, GmbH (formerly Henschel Flugzeug-Werke, GmbH) more than a decade ago. This represented a breakthrough in rotor control technology. Originally, the actuators were designed for individual blade tracking control. As the program progressed, however, the bandwidth of the actuators was steadily increased. By 1990, a flight-worthy set of actuators was available for introducing 2P to 6P IBC harmonics (nP means "n" cycles per rotor revolution). The first flight test introduced ±0.24 deg of IBC on a BO 105 helicopter in

1990. This was followed by a second test in 1991 in which the control authority was increased to ±0.49 deg. Although the initial flight test indicated vibration and noise reductions using IBC, the limited thrust and speed of the aircraft, combined with the safety-imposed low authority of the actuators prevented an exploration of the full potential of the IBC system [Refs. 15 and 16]. For this reason, a full-scale wind tunnel test program was proposed using the NASA Ames 40- by 80-Foot Wind Tunnel and a new IBC system. The new system was designed to have an even higher control authority and increased frequency response than the flight test version. The interested reader is referred to Ref. 17 for a full discussion of the plans and preparations made to support the development of this hardware for the wind tunnel testing, and to Ref. 18 for a complete description of the IBC hardware.

In the spring of 1993, the first of two proposed IBC wind tunnel tests was conducted. An extensive database was acquired during the test which included rotor performance data, vibratory hub force and moment data, blade loads data, control system loads data, inboard and outboard blade pitch motion data, and microphone (BVI noise) data. This paper presents an overview of that database and a brief description of the IBC test hardware.

Test Hardware

The IBC test was performed at the NASA Ames 40- by 80-Foot Wind Tunnel. The four-bladed, BO 105 rotor was mounted on the NASA/U.S. Army Rotor Test Apparatus (RTA) which uses two, 1500 HP electric motors to power the rotor. The RTA has a rotor balance to measure the static and dynamic rotor hub loads. Figure 1 shows the RTA and rotor installed in the test section. The test section of this closed-circuit wind tunnel is treated with sound absorptive material to allow near-anechoic acoustic measurements down to 500 Hz.

The RTA was modified for the IBC test to permit the transfer of hydraulic fluid to the IBC actuators in the rotating system. For this purpose, ZF Luftfahrttechnik specified the design of a hydraulic slipring and manufactured new hub attachment hardware to allow passage of the hydraulic supply and return lines to the IBC actuators. The general arrangement of the IBC system on the RTA is shown in Fig. 2. The 3000 psi hydraulic fluid for the IBC actuators was routed from the wind tunnel model support struts to a hydraulic control block mounted inside the RTA. This control block contained the emergency shutoff valves and the pulsation dampers (accumulators) needed to regulate the hydraulic supply pressure. From this control block, hydraulic lines were routed to a hydraulic slipring which connected the hydraulics to supply and return pressure lines in the rotating system.

The RTA main rotor shaft has a 3-in inner diameter clearance throughout its length. Originally, this space was

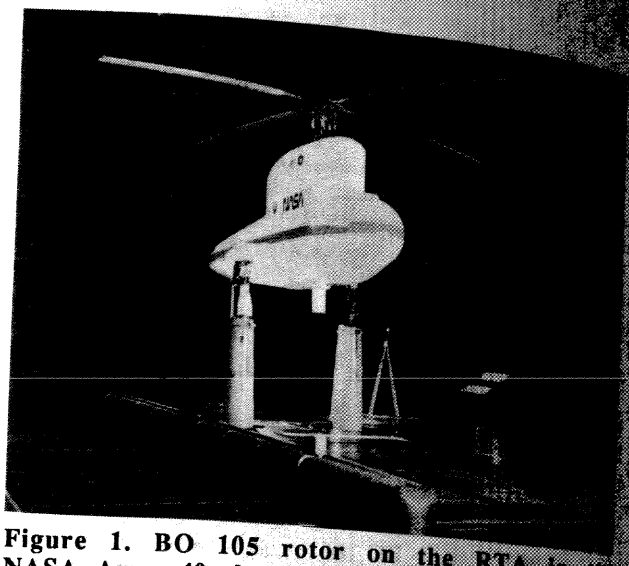

Figure 1. BO 105 rotor on the RTA in the NASA Ames 40- by 80-Foot Wind Tunnel.

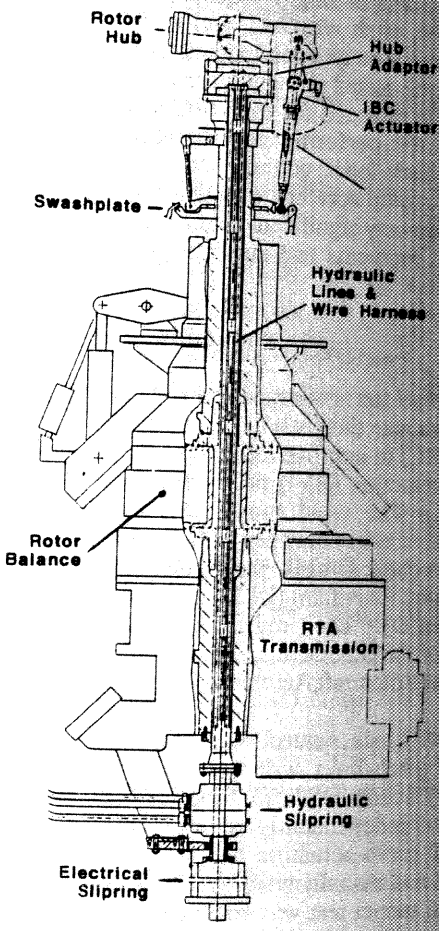

Figure 2. IBC system hardware arrangement as installed on the RTA.

used as a passageway for instrumentation wires from the rotating system transducers to an electrical slipring mounted to the lower end of the rotor shaft underneath the RTA transmission. For the IBC test, this space was fully utilized to allow passage of not only the rotating instrumentation wires, but also the hydraulic lines going to the rotor hub. The hydraulic slipring, which was mounted between the lower rotor shaft and the electrical slipring, also had a center clearance hole for the wires going to the electrical slipring. A new rotor hub adapter, which served to connect the rotor hub to the RTA rotor shaft adapter, allowed distribution of hydraulic lines to each of the IBC actuators. The hub adapter also served to support the entire weight of the hydraulic pipes, hydraulic slipring, electrical slipring, and phototach assemblies in order to provide a single-load-path through the rotor balance. Journal bearings positioned near the hydraulic slipring were used to provide centering alignment, but carried no load in the vertical direction.

Figure 3 shows an IBC actuator schematic and Fig. 4 shows the IBC actuators installed in the rotor control system. The IBC actuators connected the blade pitchhorn to the rotating swashplate. The upper and lower rod ends were the same as those used for the conventional BO 105 pitchlinks. The upper actuator housing contained the working cylinder and safety centering mechanism. The lower housing contained two LVDTs to measure actuator displacement and a strain gage to measure the actuator axial (pitchlink) force. The actuators were designed to operate under a centrifugal load of 40 g. References 17 and 18 provide a discussion of the actuator characteristics and the automatic emergency shutdown features used to maintain system safety. Figure 5 presents a plot of the maximum pitch deflection measured in bench testing as a function of the commanded input frequency. The maximum displacement of the IBC actuators during the wind tunnel test was limited to ±1.2 deg in order to avoid fatigue damage of the existing and unmodified swashplate and rotating scissors.

The IBC actuators were controlled by a computer-based controller developed by ZF Luftfahrttechnik, GmbH. Two separate subsystems were used to compute the control inputs, thereby reducing the possibility of uncontrolled actuator travel. Each subsystem received an independent measurement of actuator displacement from one set of LVDTs (two LVDTs per actuator). Both subsystems also received the user-specified IBC command (phase and magnitude for up to 12 harmonics) from a personal computer (PC). Using this information, each subsystem computed the actuator controls. Although only the commands from one subsystem was sent to the actuator servo-valves, both subsystems monitored the displacement of each of the four actuators for position errors. Either subsystem could lock-out the IBC actuator motion in the event of an emergency stop of the wind tunnel, loss of rotor RPM, loss of hydraulic pressure, actuator position error, or excessive axial force on any one of the four actuators.

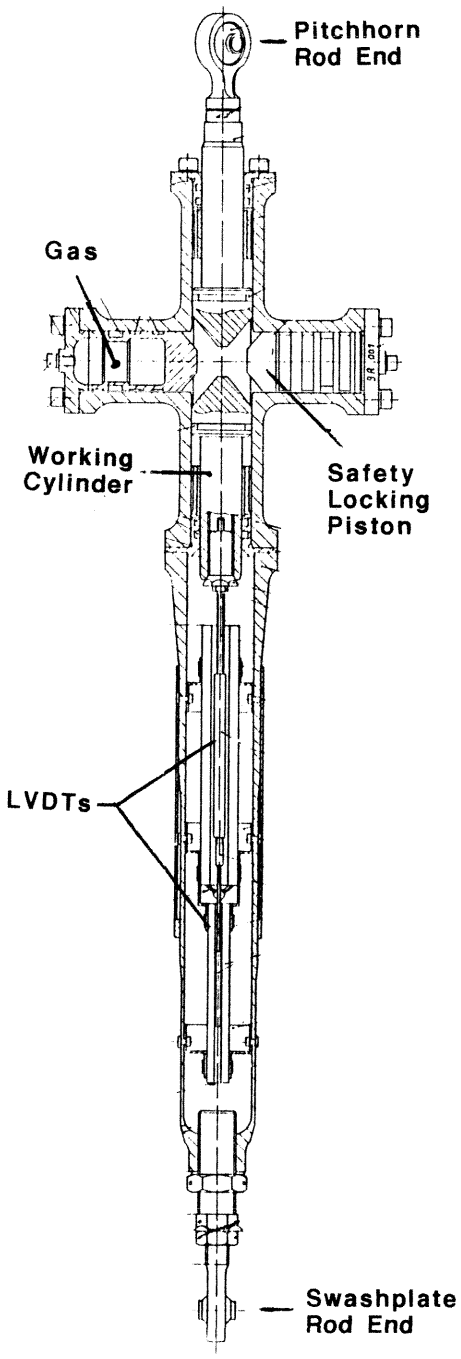

Figure 3. Schematic of the IBC actuator.

Test Matrix

Single frequency harmonics of 1P-12P were introduced without blades to assess the control system inertial forces. These tests were repeated with blades installed for input harmonics up to 6P. Single harmonic inputs of 2P - 6P

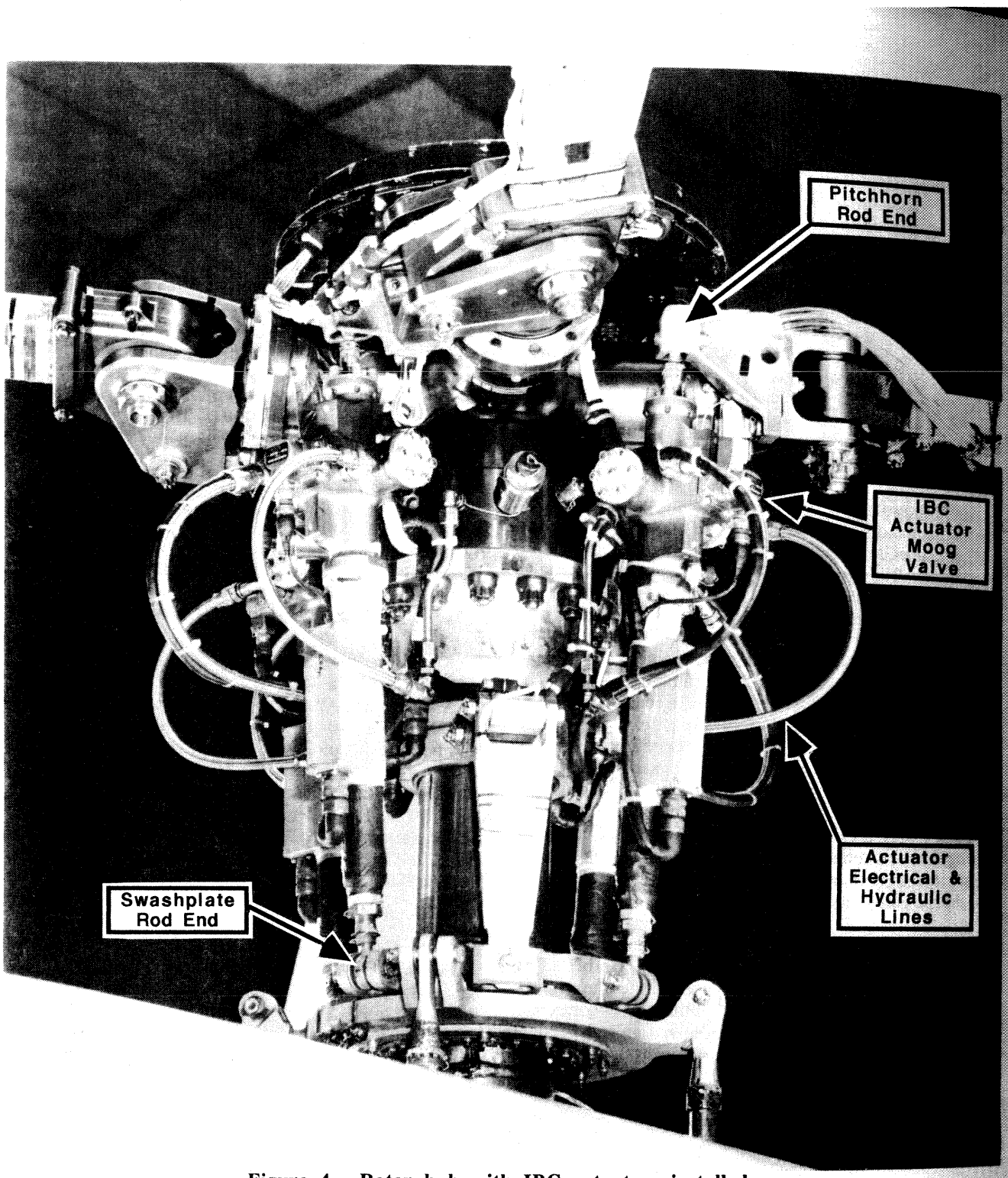

Figure 4. Rotor hub with IBC actuators installed.

were extensively studied at several conditions to evaluate their effects on performance, vibration, and noise. Table 1 presents the test conditions and IBC control amplitudes for the single-frequency IBC inputs. The reason for relatively few flight conditions was to maximize the number of IBC controls evaluated within the allowed test time. At the 43 kt and 127 kt conditions, data were acquired for both minimized flapping and prescribed moment trims. IBC inputs at the 43 kt condition were extensively studied because of the high vibration levels produced at that condition. At the 64 kt condition, the rotor shaft was tilted aft to establish a condition producing relatively high BVI

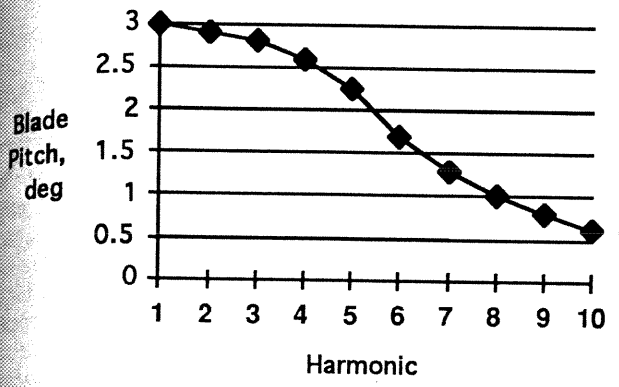

Figure 5. IBC actuator frequency response.

noise. For most data points, the rotor thrust was selected to simulate a 1g level flight condition ($C_T/s \approx 0.07$). However, at 85 kts, the thrust was considerably higher ($C_T/s \approx 0.12$). The single-frequency harmonic of most interest was the 2P input for its effect on rotor performance, noise, and vibration. In most cases, the IBC control input phase was changed in either 30 deg or 60 deg increments for a full 360 deg of control input phase angle. The pitch equations for IBC input are given by

$$\theta_i = AMP * Cos\left[n\left(\Psi_1 - (i-1)(90\,\text{deg})\right) - \phi\right] \quad (1)$$

where θ_i is the pitch of the i^{th} blade, Ψ_1 is the rotor azimuth angle of blade 1 (as shown in Fig. 6), and ϕ is the

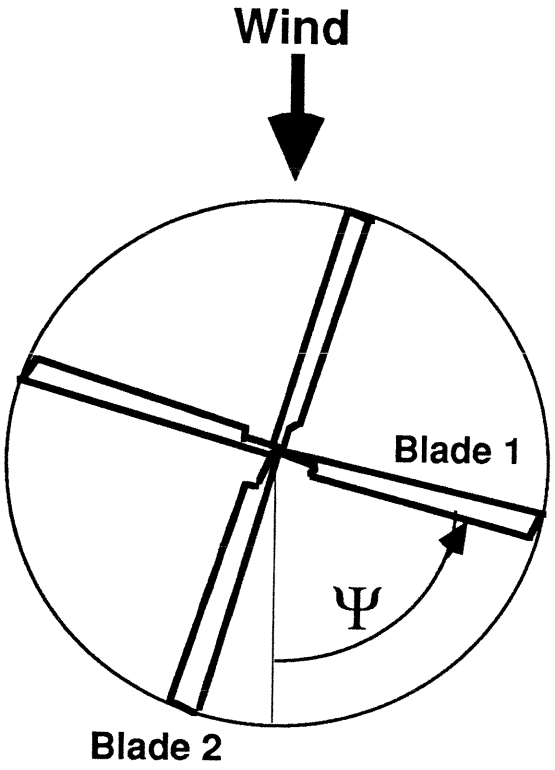

Figure 6. Definition of rotor azimuth angles and blade numbers.

Table 1. Test conditions and amplitudes for single-frequency IBC excitation.

	Tunnel Speed, kt (advance ratio)					
Harmonic Input	Hover (0.00)	43 (0.10)	64 (0.15)	85 (0.20)	127 (0.30)	150 (0.35)
2 P	±0.5 deg ±1.0 deg	±0.5 deg ±1.0 deg	±1.0 deg ± 1.2 deg	±1.0 deg	±1.0 deg ± 1.2 deg	±1.0 deg
3 P	±0.5 deg ±1.0 deg	±0.5 deg ±1.0 deg	±1.0 deg		±1.0 deg	
4 P	±0.5 deg ±1.0 deg	±0.5 deg			±1.0 deg	
5 P	±0.5 deg ±1.0 deg	±0.5 deg ±1.0 deg			±1.0 deg	
6 P	±0.5 deg ±1.0 deg	±0.5 deg ±1.0 deg	±1.0 deg			

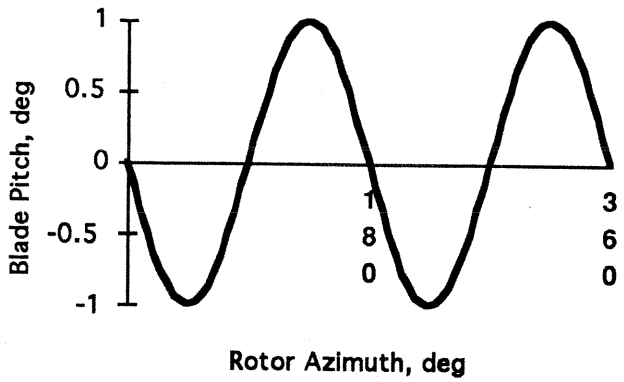

Figure 7. 2P IBC control at 270 deg input phase angle.

IBC control phase angle. The (i-1)*(90 deg) phase shift insures that all of the four blades follow the same pitch rotation as they traverse the azimuth. A 2P input with a phase angle of 270 deg is shown in Fig. 7. As seen in that figure, the 2P cosine waveform has been shifted 270 deg of a 2P period to the right.

The strength of the IBC system lies in its ability to generate blade pitch schedules which ordinary HHC applied through the swashplate cannot achieve. For rotors having 4 blades, IBC allows 2P and 6P excitation, in addition to the 3P, 4P, and 5P excitation which can be introduced through the conventional swashplate. Moreover, using combinations of harmonics 2P - 6P, pitch schedules such as pulses and wavelets can be created through Fourier synthesis. Figure 8 shows the harmonic amplitudes and phase angles required to generate the negative blade root pitch pulse. Such waveforms were tested in the BVI noise reduction studies. This change in root pitch, however, was not a pulse at the blade tip because the blade torsional dynamics (first mode at about 3.6P) changed the magnitude and phase of the IBC

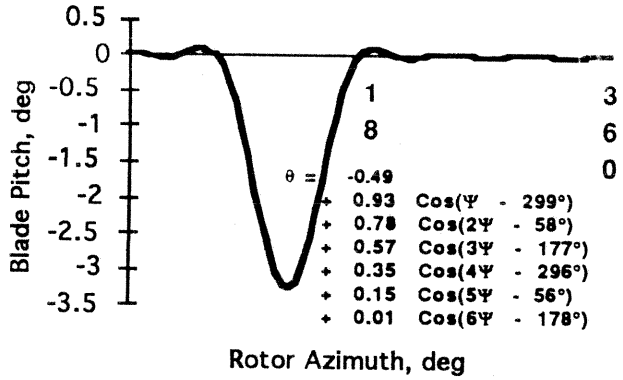

Figure 8. Combination of harmonics 1 to 6 to form negative pulse at blade root.

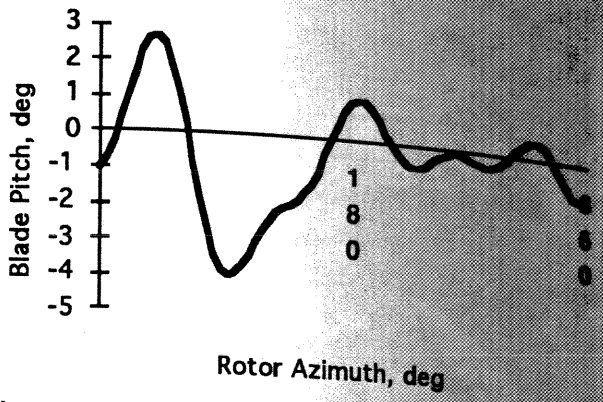

Figure 9. Negative Wavelet at 120 deg.

input from root to tip. These magnitude and phase shifts were calculated from the blade tip accelerometer data obtained at the 43 kt test condition. The blade root pitch control schedule shown in Fig. 9 was required to generate the pitch pulse shown in Fig 8 at the blade tip. This root pitch input was called a wavelet. Similarly, a doublet was the root pitch input required to produce two pulses (either positive or negative) at the blade tip.

Table 2 presents the test conditions and IBC control amplitudes for the multi-frequency inputs tested. Although some combinations of 2-3-4-5P harmonics were tried for vibration control at 43 kts and 127 kts, most of the multi-harmonic input was to generate pitch schedules specifically for BVI noise reduction.

Table 2. Test conditions and amplitudes for multi-frequency IBC excitation.

	Tunnel Speed (advance ratio)		
IBC Input	43 kt 0.10	64 kt 0.15	127 kt 0.30
2 - 3 - 4 - 5	±1.0 deg		±1.0 deg
+ Pulse		±1.0 deg	
- Pulse		±1.0 deg	
+ Wavelet		±1.0 deg	
- Wavelet		±1.0 deg	

Instrumentation

The BO 105 rotor used for the wind tunnel test was instrumented as indicated in Table 3. Strain gages were used to measure blade bending moments during IBC excitation. In addition to measuring the change in blade torsional loads with IBC, the torsional strain gages were also used to help assess the IBC input phase shift from the blade root to blade tip produced by the blade torsional dynamics. The IBC input amplitude attenuation from blade root to blade tip and phase shift at the tip were calculated from miniature accelerometers at the blade tip. Miniature, surface-mounted pressure transducers were also used to measure the pressure at four leading edge blade locations. These were positioned on the upper blade surface to detect the presence and location of blade-vortex interactions. The BVI location information could be used to suggest possible wavelet and doublet IBC pitch schedules for BVI noise control.

The RTA five-component rotor balance was used to measure the rotor thrust, side force, drag force, pitching moment and rolling moment. Both steady and dynamic loads were measured. The dynamic measurements were used to assess the effect of IBC on the vibratory hub loads. Rotor power was calculated from the shaft torque measurement obtained from the flex-coupling located between the upper and the lower rotor drive shafts.

Table 3. Instrumentation.

Measurement	Location
Rotor Blade:	in from center, (R=193.2 in)
Blade Flap Bending Moment	20
Blade Chord Bending Moment	28
Blade Torsion Moment	65, 77, 110, 155
Blade Pressures	116, 135, 155, 174
Blade Accelerometers	58, 97, 135
Blade Tip Accelerometers	Leading Edge, Flap Trailing Edge, Flap
Rotor Balance: (also wind tunnel scales)	Lift, Side, and Drag Forces Pitching and Rolling Moments
Flex-coupling	Shaft Torque
Control System:	
IBC Actuator Position	8 (2 LVDTs per Actuator)
IBC Actuator Forces	4
Swashplate Position	1 (LVDT per Control Rod)
Swashplate Control Rod Forces	3
Blade Pitch Transducers	4 (1 per blade)
Microphones:	
Stationary	1, retreating side
Traverse	2

The displacements and forces of both the stationary swashplate control actuators and the IBC actuators were measured. Each IBC actuator had two LVDTs to provide a dual position measurement for each IBC actuator. Loads on the control system were evaluated by measuring the axial force (or pitchlink load) developed in each of the four IBC actuators and each of the three control rods holding the swashplate attitude. In addition, the root pitch of each blade was measured using resistive strips at the pitch bearing.

Acoustic data was recorded using two moving microphones below the advancing side and a fixed microphone below and aft of the retreating side. The advancing side microphones were fixed in the lateral and vertical directions and moved by a traverse in the streamwise direction under the rotor. Figure 10 shows the microphone and traverse positions. Because data acquisition with the traverse was time-consuming, only a single position of the traverse was used for most data points. However, to document the baseline noise levels and directivity with IBC inputs producing substantial BVI noise reductions, the traverse was moved to acquire data from 6 positions under the rotor. These positions are also indicated in Fig. 10.

Data Reduction

A zero or reference point reading was obtained prior to the start of each wind tunnel data run. These zero values were subtracted from the raw data obtained during the run. The reference point was defined as the rotor collective pitch set to 10.6 deg, the IBC hydraulics turned on, and the wind speed, rotor shaft angle, rotor RPM, and cyclic pitch all set to zero.

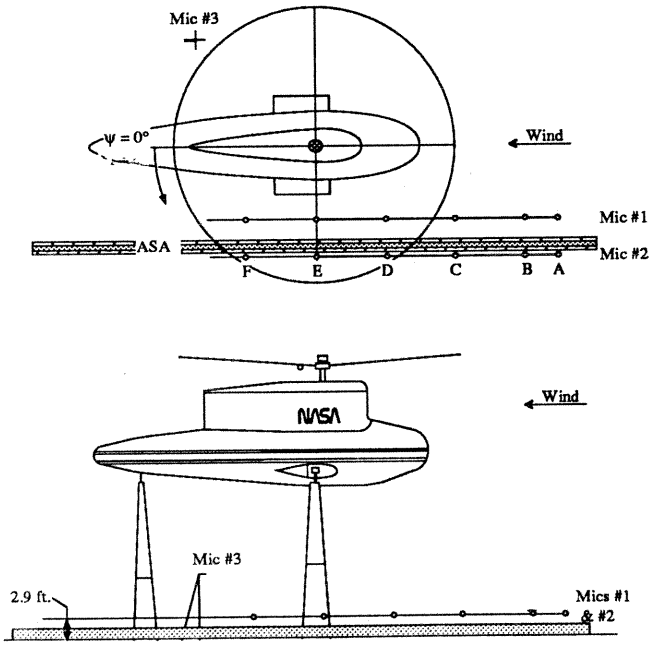

Figure 10. Microphone and traverse positions

The rotor balance and wind tunnel scale data were corrected to account for weight changes due to variations in the rotor shaft angle. A weight tare data set was obtained with the wind off, acquiring data throughout the shaft angle range and then curve-fitting the result for the rotor force and moment data. The curve fit was subtracted from the test data at each point. Similarly, to eliminate the effects of control system drag on the rotor forces and moments, aerodynamic tare data were acquired at a number of airspeeds with the swashplate, hub, and IBC actuators installed. The data were also curve fitted and subtracted from the rotor forces and moments data.

Depending on the instrumentation transducers, either static data, dynamic data, or both were acquired. The static data represented values averaged over 15 rotor revolutions. The dynamic data were time histories sampled at 64/revolution or about 453 Hz. Both original and averaged time histories were available from the dynamic measurements.

IBC Test Data

IBC Blade Motion

One of the most fundamental questions answered during the IBC test was whether or not the proposed system would impart the desired IBC motions to the blade. On the one hand, it was uncertain how accurately the IBC actuators would follow the commanded signals. Another issue was how accurately the actuator stroke would be transformed into blade pitch motions. The former question regarded the IBC system controller, whereas the latter depended mainly on the control system stiffness and the effect of the blade torsional dynamic response.

Comparison of commanded and measured stroke amplitudes for IBC inputs 2P through 6P showed that the IBC controller worked quite well. The transformation of actuator stroke into pitch angle was found to be very repeatable, with one millimeter of actuator stroke producing 0.34 deg of blade pitch at the root. The one exception was for input at 4P IBC excitation, which produced a loss of about 18 percent. The reason was that at 4P, all four of the actuators were moving together in phase, causing a vertical vibration of the swashplate assembly.

The most accurate transformation, even for inputs smaller than ±1 mm, was achieved for 2P and 6P inputs. At these frequencies, the IBC actuator forces canceled each other in the rotating system, so that virtually no 2P or 6P control loads were transmitted to the stationary frame.

The accuracy of the IBC motion fell for inputs less than ±0.5 deg amplitude. This was probably the result of lost motion in the control system amounting to about 0.1 deg.

Prior to the IBC test, it was recognized that the blade torsional dynamics (first mode about 3.6P) would alter the IBC input magnitude and phase from blade root to blade tip. For this reason, miniature accelerometers were installed at the blade tip in order to calculate the torsional motion at this blade tip (Fig. 11). As shown in Ref. 19, if signals from these accelerometers are summed, the resulting signal is given by

$$\frac{\left(a_{nLE}+a_{nTE}\right)}{R\Omega^2}=\frac{1}{R}\left(l_{LE}+l_{TE}\right)\theta_n\left(1-n^2\right) \qquad (2)$$

where n is the IBC input harmonic number, a_{LE} and a_{TE} are the leading edge and trailing edge acceleration (Fig. 11), and θ_n is the n^{th} harmonic of the pitch at the blade tip. The amplitude of the n^{th} IBC harmonic at the blade tip, $AMP_{\theta n}$, is therefore

$$AMP_{\theta n}=\frac{\left(a_{nLE}+a_{nTE}\right)}{\left(l_{LE}+l_{TE}\right)\left(\Omega^2-(n\Omega)^2\right)} \qquad (3)$$

and the phase shift of the n^{th} harmonic at the blade tip, $\phi_{Tip,n}$, is

$$\varphi_{Tip,n}=\arctan\left(\frac{\left(a_{nLE,S}+a_{nTE,S}\right)}{\left(a_{nLE,C}+a_{nTE,C}\right)}\right) \qquad (4)$$

where the subscripts S and C denote sine and cosine Fourier series coefficients of blade tip acceleration. The magnitude and phase shifts thus computed from the tip accelerometers are presented in Table 4.

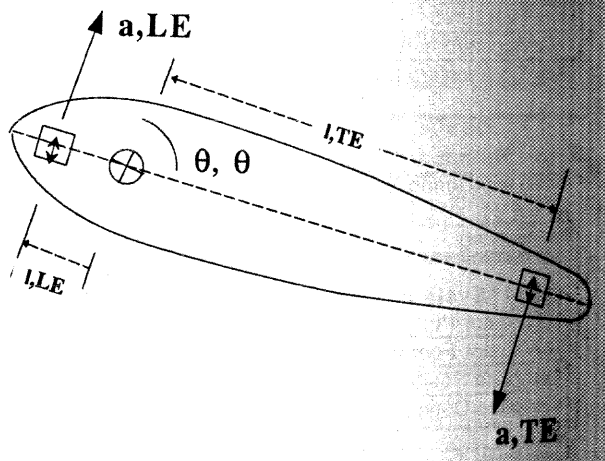

Figure 11. Position and sensing direction of accelerometers located at the blade tip.

Table 4. IBC magnitude and phase shifts produced by blade torsional dynamics.

IBC Root Input	Amp. at Blade Tip	Phase Lag, deg Ψ	Phase Lag, deg nP
2 P	0.60	-10 deg	-20 deg
3 P	0.50	-13 deg	-39 deg
4 P	0.58	-33 deg	-132 deg
5 P	0.21	-42 deg	-210 deg
6 P	0.15	-34 deg	-204 deg

Vibratory Hub Loads

The effect of IBC on rotor vibration was evaluated using the oscillatory hub loads acquired from the rotor balance. The 43 kt condition was studied because it exemplified the high vibration found in the transition region between hover and forward flight. For this study, the rotor was trimmed to minimize 1P flapping. Because the BO 105 rotor was four-bladed, the 4P vibration component was the largest. Figure 12A shows a large 4P hub pitching moment for the case of no IBC excitation at the 43 kt flight condition. The dominant 4P vibration was also seen in the other rotor balance forces and moments. Further, as shown in Fig. 12B for ±1.0 deg, 3P IBC input at 90 deg phase angle, the rotor hub vibrations remained dominated by the 4P component with IBC excitation. This was true for the other rotor hub forces and moments as well, with few exceptions.

In the plots which follow, the effect of IBC on the 4P hub forces and moments is presented for IBC inputs of 2P through 6P at the 43 kt high vibration condition. The 4P inplane hub shear force magnitude was computed as the vector sum of the drag and side forces. Similarly, the 4P hub bending moment was computed as the vector sum of the pitching and rolling moments. However, the moments and forces of the RTA rotor balance were not frequency response corrected to account for dynamic amplification or attenuation of the balance outputs. Since the 4P pitching moment measured by the balance was sometimes as much as 3 to 4 times the theoretical aircraft shaft bending limit (15,000 - 20,000 ft-lbs), the dynamic corrections, when made, will have large effects. At this time, calibration of the rotor balance to account for all of the interactions is yet in progress [Ref. 20]. Nevertheless, the effect of IBC on the trend of the 4P hub forces and moments relative to the baseline (no IBC) condition is held to be valid, even though the absolute magnitude of the forces and moments may be in error.

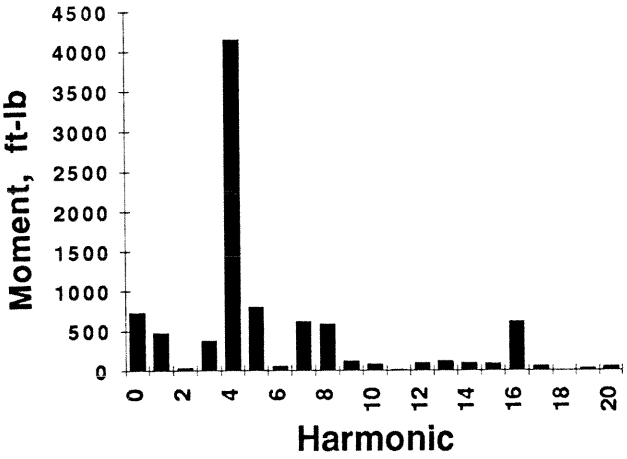

Figure 12A. Pitching Moment at 43 kts without IBC.

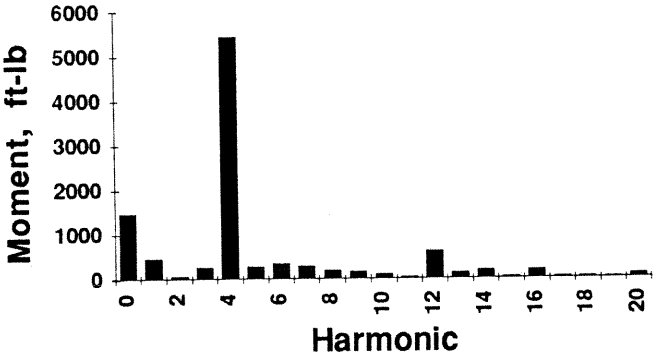

Figure 12B. Pitching Moment at 43 kts with ±1.0 deg 3P IBC input at 90 deg phase angle.

The effect of ±0.5 deg and ±1.0 deg of 2P IBC excitation on the 4P hub forces and moments at the 43 kt condition is presented in Figs. 13A and 13B, respectively. The 4P lift, 4P in-plane shear force, and 4P bending moment were reduced or amplified simultaneously, depending on the phase of the 2P IBC input. The effect of doubling the IBC pitch amplitude was roughly to double the amount of reduction in the 4P forces and moments. The highest reductions in the 4P hub loads occurred at a 2P phase angle of 60 deg.

Figures 14A and 14B show the effect of 3P IBC on the 4P hub vibrations using input amplitudes of ±0.5 and ±1.0 deg, respectively. In a manner similar to the effect seen for 2P IBC, the 4P hub lift, 4P hub shear force, and 4P hub bending moment were reduced or amplified as the phase of the 3P input was varied. At ±1.0 deg and a phase of 150 deg, Fig. 17 shows nearly complete suppression of the 4P lift force and about 50 percent reduction of the 4P hub shear force and 4P hub bending moment.

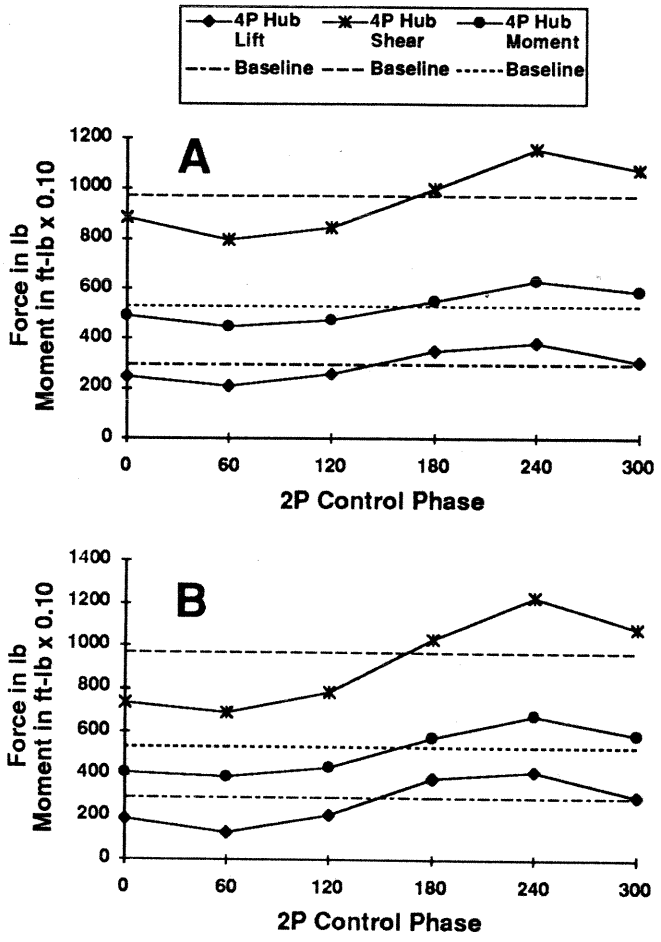

Figure 13. Effect of 2P IBC on 4P hub loads at 43 kt with minimum 1P flapping trim: A) ± 0.5 deg, B) ± 1.0 deg.

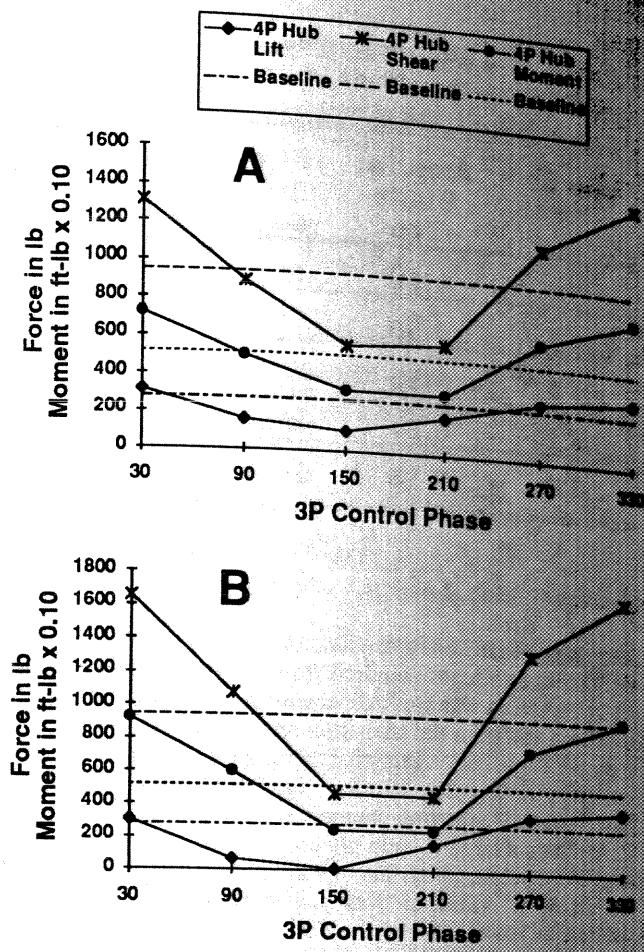

Figure 14. Effect of 3P IBC on 4P hub loads at 43 kt with minimum 1P flapping trim: A) ± 0.5 deg, B) ± 1.0 deg.

The 4P IBC input at 43 kt could not be introduced with ±1.0 deg amplitude because of high loads developed in the primary control system. Nevertheless, Fig. 15 shows that for even ±0.5 deg of 4P IBC input that the rotor hub 4P forces and moments were significantly reduced. In fact, the reductions were almost as large as that seen using ±1.0 deg of 3P excitation. The optimal phase angle for 4P input was 240 deg to minimize the 4P in-plane forces and hub moments. The 4P vertical forces was best minimized at 300 deg.

Figures 16A and 16B show that the 5P IBC inputs had little or no beneficial effect on the 4P hub vibrations at the 43 kt flight condition. At most phase angles, 5P input increased the oscillatory hub loads from the baseline values. For ±0.5 deg input, a slight reduction in all five hub forces and moments was achieved at a 5P input phase angle of 30 deg.

Figures 17A and 17B show that the 6P IBC inputs usually increased the 4P hub vibrations at the 43 kt flight condition. Although the 4P hub oscillatory lift force was slightly

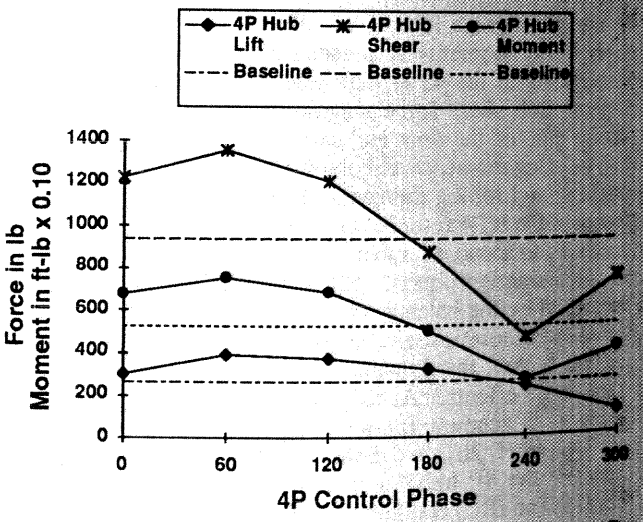

Figure 15. Effect of ± 0.5 deg 4P IBC on 4P hub loads at 43 kt with minimum 1P flapping trim.

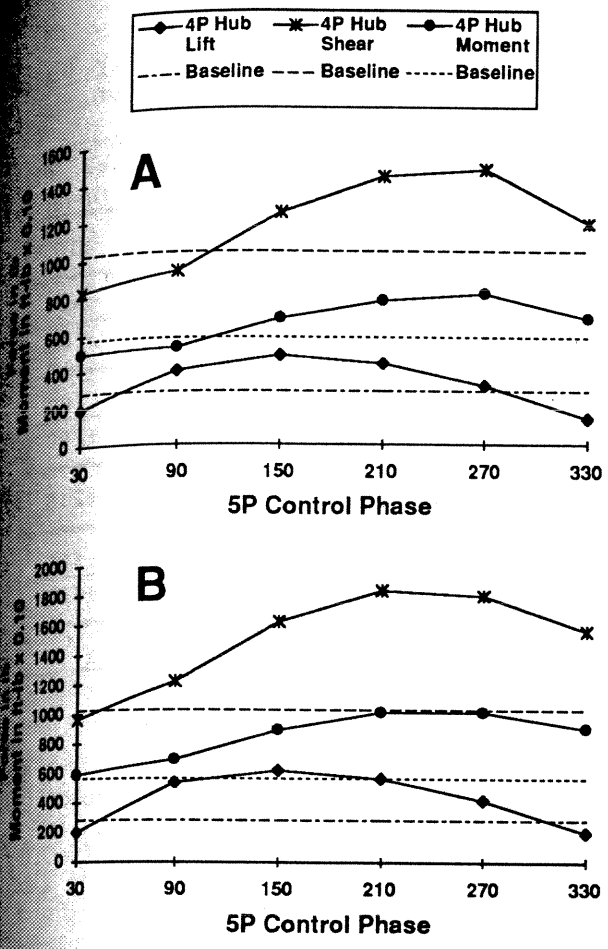

Figure 16. Effect of 5P IBC on 4P hub loads at 43 kt with minimum 1P flapping trim: A) ± 0.5 deg, B) ± 1.0 deg.

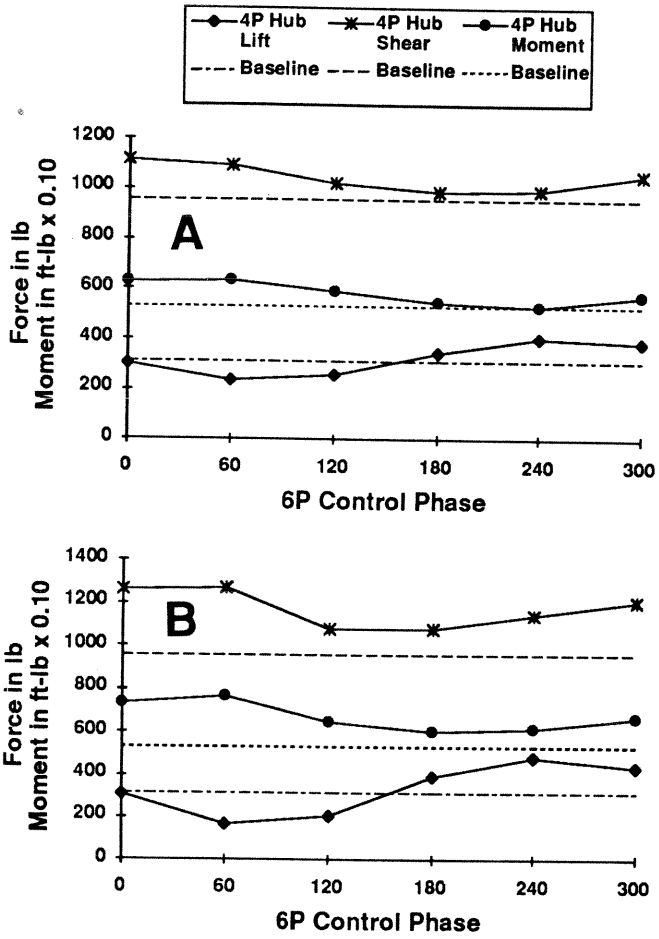

Figure 17. Effect of 6P IBC on 4P hub loads at 43 kt with minimum 1P flapping trim: A) ± 0.5 deg, B) ± 1.0 deg.

duced at a few phase angles, there was no 6P input which duced all 5 components of the rotor balance outputs at ce.

or all of the IBC inputs tested at 43 kt and ±0.5 deg and 1.0 deg amplitude, it was seen that raising the amplitude d not change the phase angles of best vibration reduction r each of the IBC harmonics. The changes in the 4P hub rces and moments with IBC input amplitude indicated the stem to be fairly linear with IBC input magnitude.

ne conclusion gained from the data at 43 kt was that nerally all of the rotor balance forces and moments were fected in a similar fashion as a function of the IBC input ase angle. Hence, a vibration controller designed to ppress only 4P hub pitching moment would likely also ppress all of the other 4P hub forces and moments at the me time. If valid at higher airspeeds, this would mean a nsiderable reduction in the state description needed to aracterize the vibration state.

Blade Loads

The effect of IBC on blade loads was examined for the 43 kt flight condition with the rotor trimmed to minimize 1P blade flapping. The data for ±0.5 deg and ±1.0 deg IBC excitation displayed similar trends as the IBC phase angle was varied.

IBC did not have a substantial effect on the mean flap bending moment and the mean torsion moment. However, the mean chord bending moment was slightly affected by 2P and 3P IBC inputs, as shown in Figs. 18A and 18B. It was found that 3P inputs generally resulted in a reduction of the mean chord bending moment, with a maximum of 8 percent reduction. The 2P inputs caused reductions of about 3 percent as well as increases of about 5 percent, depending on the IBC phase angle. These increases and decreases in mean blade loads are not large and could simply be the result of re-trimming the rotor to minimize the 1P flapping.

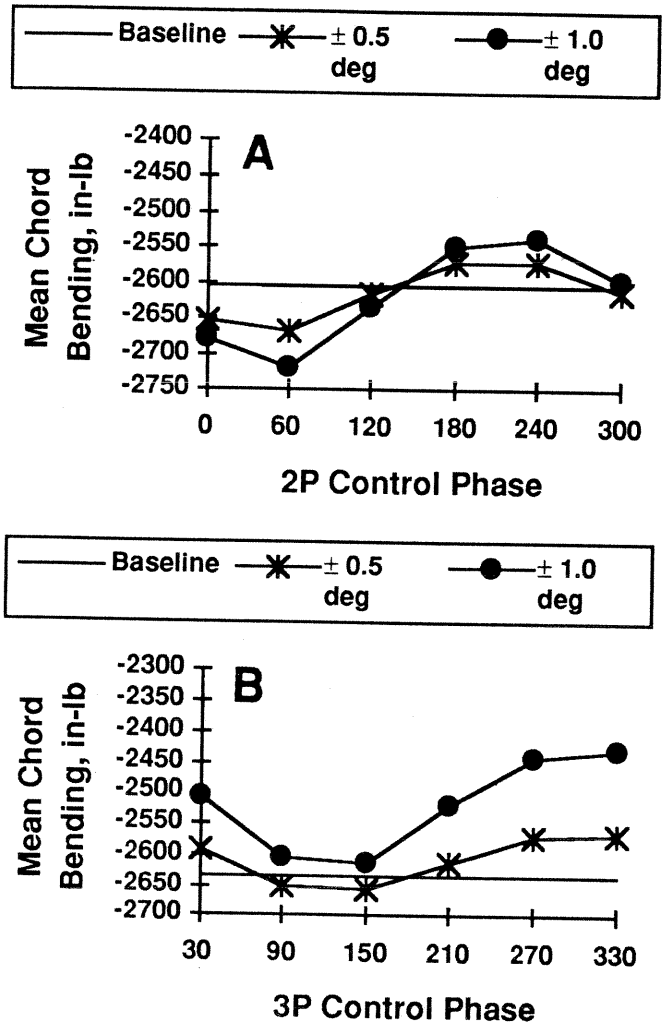

Fig 18A. Effect of IBC on mean chord bending at station 110.0: A) 2P, B) 3P.

The most significant effect of IBC on oscillatory blade loads was an increase in the oscillatory torsion moment for all IBC inputs tested. As expected, the loads increased with increased IBC amplitude. Fourier analysis of the blade torsional strain gages showed that the harmonic most largely effected corresponded to the IBC input frequency. Table 5 presents the nP torsional loads at 40 percent, 57 percent, and 80 percent radial station produced by nP IBC excitation. The effect on torsional loads other than nP was negligible In most cases, doubling the excitation from ±0.5 deg to ±1.0 deg doubled the torsional moment.

IBC also showed a large effect on the oscillatory flap bending moments (Fig. 19). The 2P and 3P inputs resulted in slight reductions at one phase angle and substantial increases of up to 100 percent at the other phase angles, as shown in Figs. 19A and 19B. Figure 19C shows that ±0.5 deg 4P IBC input caused a reduction of about 15 percent at 300 deg phase angle, and an increase of about 25 percent at

Table 5. Torsional oscillatory blade loads with IBC excitation.

IBC Excitation	0.40 r/R (in-lb)	0.57 r/R (in-lb)	0.80 r/R (in-lb)
Baseline	±40	±20	±15
2P, ±0.5 deg	±90	±70	±55
2P, ±1.0 deg	±170	±135	±105
3P, ±0.5 deg	±235	±175	±100
3P, ±1.0 deg	±435	±345	±200
4P, ±0.5 deg	±430	±365	±215
5P, ±0.5 deg	±355	±315	±185
5P, ±1.0 deg	±705	±625	±380
6P, ±0.5 deg	±305	±285	±175
6P, ±1.0 deg	±605	±570	±350

120 deg input phase angle. Figures 19D and 19E show that the 5P and 6P IBC inputs increased the oscillatory flap bending moments at all input phase angles. Table 6 presents the harmonic load distribution in units of in-lb flap bending moment at blade station 20. Although it is seen that the harmonic most increased corresponded to the harmonic of IBC excitation, the other harmonics were affected as well.

All frequencies but 4P IBC had a large impact on the oscillatory chord bending moments. The most significant reduction (about 50 percent) was achieved with a 3P input of

Table 6. Harmonics of oscillatory flap bending moment at station 20 with IBC excitation (in-lb).

IBC Input*	1P	2P	3P	4P	5P	6P
No IBC	448	180	575	216	70	87
2P at 120°	1404	905	572	116	116	66
3P at 330°	242	559	1099	177	275	59
4P at 120°	584	394	783	109	101	39
5P at 270°	78	349	857	71	631	60
6P at 240°	264	111	357	370	504	324

* inputs applied at ±1.0 deg; (4P at ±0.5 deg.)

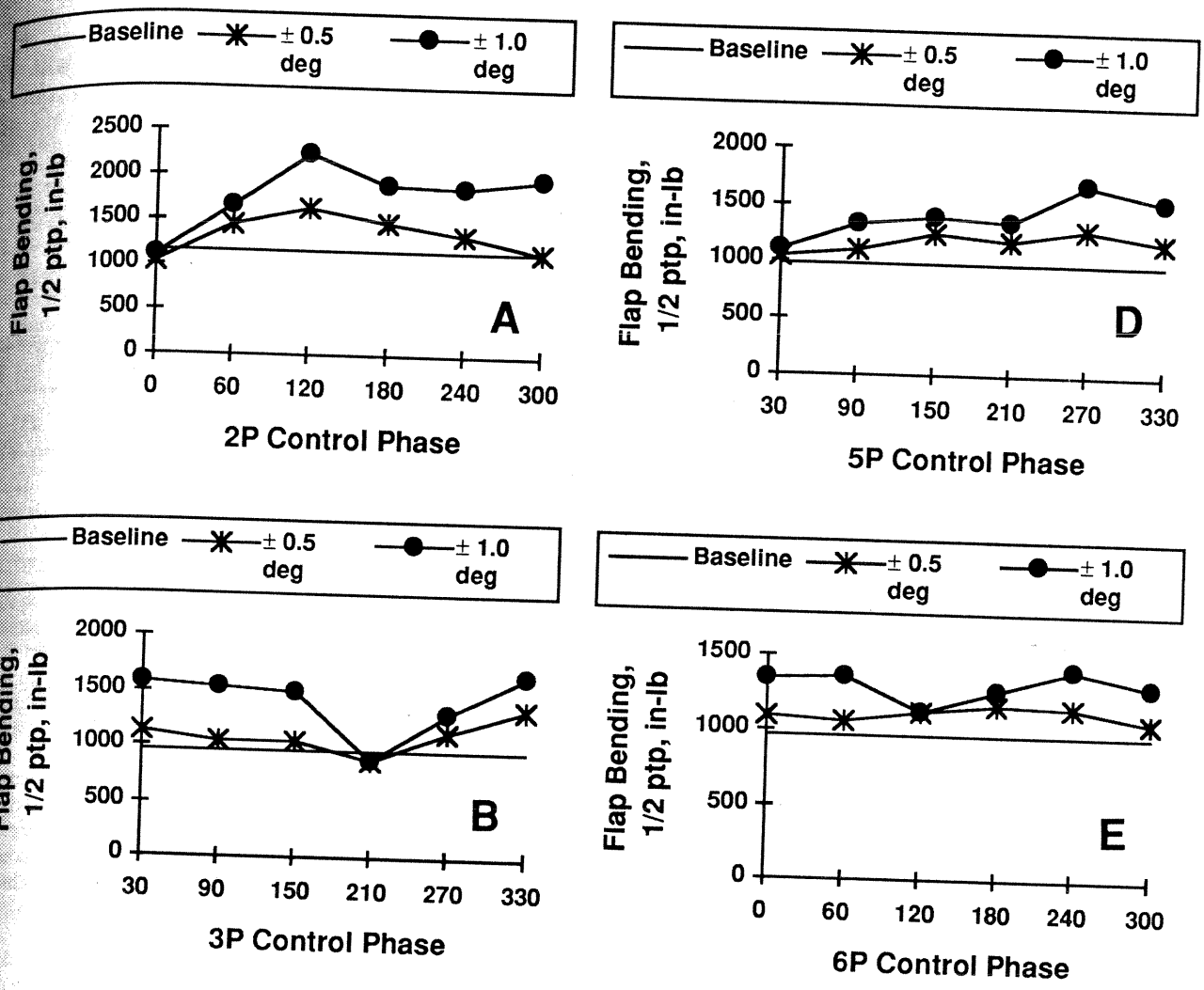

Fig 19. Effect of IBC on oscillatory flap bending at station 20.0 at 43 kt and minimum 1P flapping trim: A) 2P, B) 3P, C) 4P, D) 5P, and E) 6P.

±1.0 deg and 150 deg input phase angle, as shown in Fig. 20A. Figures 20B and 20C show that 5P and 6P IBC reduced the chord bending moment by 20 percent or increased it by 70 percent, depending on the phase angle. Table 7 presents the harmonic load distribution in units of in-lb chord bending at blade station 110. It is seen that the 3P at 150 deg achieved a load reduction by mainly reducing the 4P component. This is the same phase angle for best 4P hub load reduction using 3P IBC. Although the 5P input mostly effects the 5P chord bending, the 6P input also strongly influences the 4P chord bending loads.

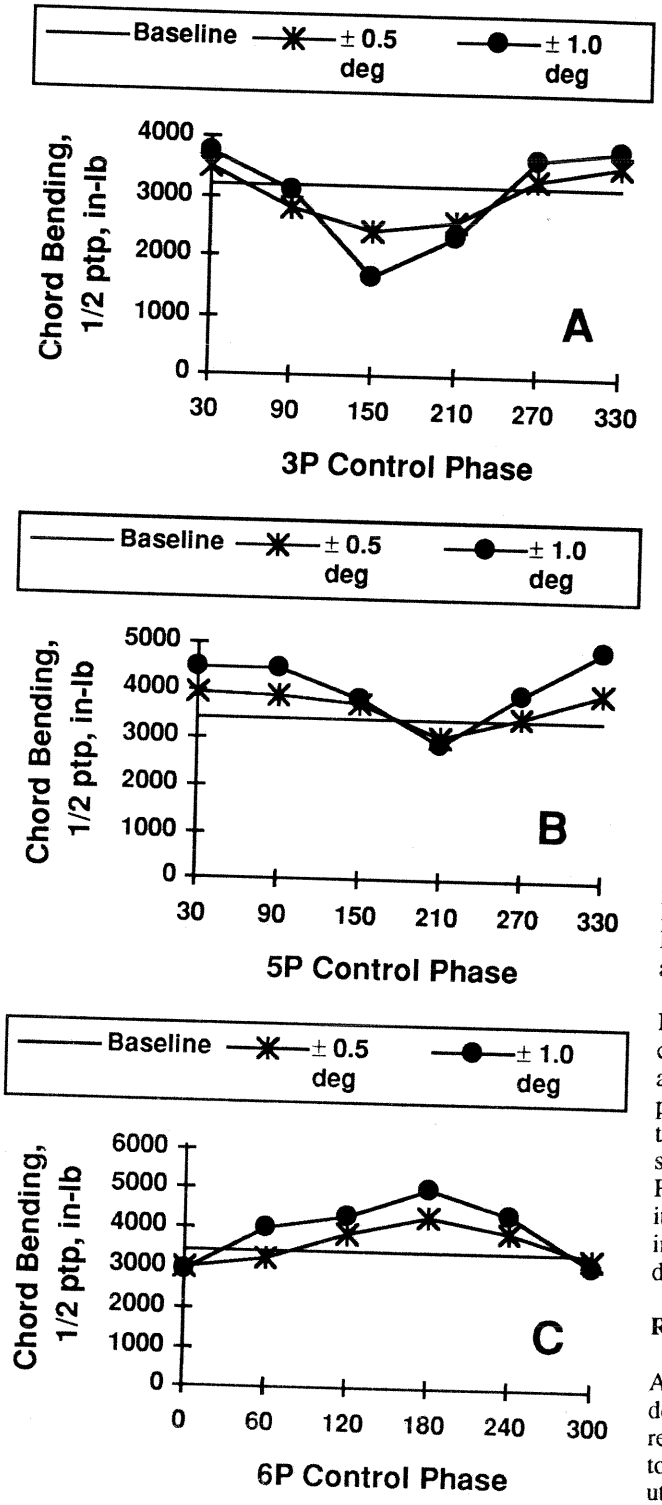

Fig 20C. Effect of IBC on oscillatory chord bending at station 110.0 at 43 kt and minimum 1P flapping trim: A) 3P, B) 5P, and C) 6P.

Table 7. Harmonics of Oscillatory Chord Bending Moment at Station 110 with IBC excitation at 43 kt and minimum 1P flapping trim (in-lb).

IBC Input*	1P	2P	3P	4P	5P	6P
No IBC	467	333	464	2304	323	17
3P at 50°	353	75	268	917	521	56
5P at 90°	684	237	288	2565	1597	76
6P at 80°	652	286	500	3376	1279	283

* All inputs applied at ±1.0 deg.

Control System Loads

To determine the influence of IBC on the control system loads, the mean and half peak-to-peak values of the actuator forces were examined. Data from the four actuators were averaged for the results presented here. Although IBC showed a negligible effect on the actuator mean forces, the half peak-to-peak values increased with IBC as shown in Fig. 21. As expected, the actuator oscillatory forces rose proportionately with IBC amplitude and as the square of the input frequency. For 2P and 3P excitation (Figs. 21A and 21B), the amount of force increase was also a function of the IBC input phase angle, but not for the other IBC harmonics. Like the oscillatory blade torsion moment, the oscillatory actuator forces were the highest for 4P input (Fig. 21A).

Inevitably, pitching the blades with IBC increased the control system loads very noticeably. Though the IBC actuators were designed to produce ±3.0 deg of blade root pitch, only ±1.2 deg of blade pitch could be achieved during the wind tunnel test before the loads reacted by the RTA test stand swashplate rose above the endurance life level. However, the upper control system of the BO 105 rotor itself would have withstood the IBC actuator force produced in this test at full-stroke without incurring any fatigue damage.

Rotor Performance Data

A major objective of the wind tunnel program was to determine the ability of 2P IBC to reduce the rotor power requirements by suppressing retreating blade stall. In order to maintain roll moment equilibrium, the helicopter must utilize increasing 1P lateral cyclic pitch input as the forward flight speed increases. This serves to increase the blade pitch on the retreating side, while decreasing the blade pitch on the advancing side. As this continues, the retreating blade becomes stalled due to the high increase in lateral

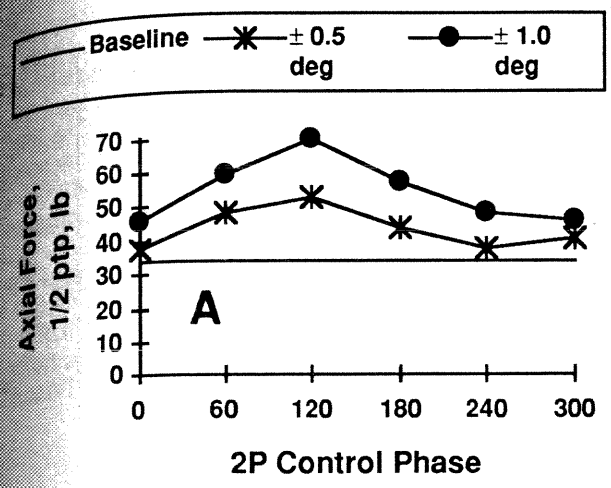

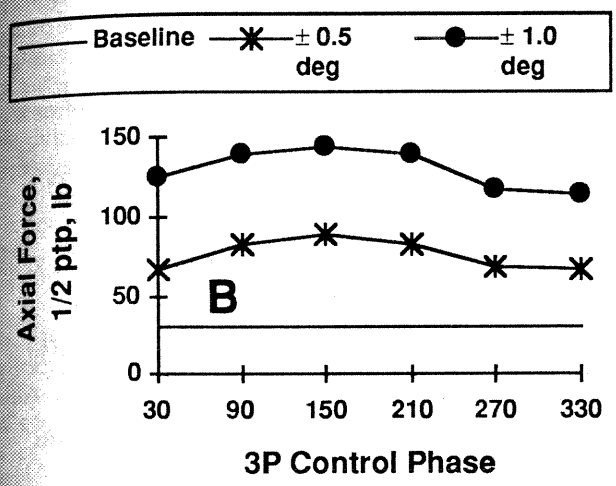

Fig 21. Effect of IBC on IBC actuator axial force: A) 2P and B) 3P.

cyclic pitch input. Using 2P control, the onset of stall might be suppressed by phasing the IBC input to reduce the blade angle of attack on both the retreating and advancing sides of the rotor, while further loading the fore and aft portions of the rotor disk. At first thought, it would seem that a small subtraction of pitch angle from both sides of the rotor (and the addition of pitch fore and aft) should not greatly change the 1P pitch and roll moment equilibrium.

However, during the IBC test it was found that input of 2P IBC did, in fact, change the trim state of the helicopter very significantly. Figure 22 shows large changes in the steady hub pitching and rolling moments produced by ±1.0 deg of 2P IBC at 127 kt with the rotor trimmed to minimize flapping. This made assessment of the effect of 2P IBC on performance very difficult, if not impossible, because the measured shaft power was influenced by changes in the rotor trim state. The variation in rotor lift and horsepower is shown in Fig. 23 for the same 127 kt flight condition. The

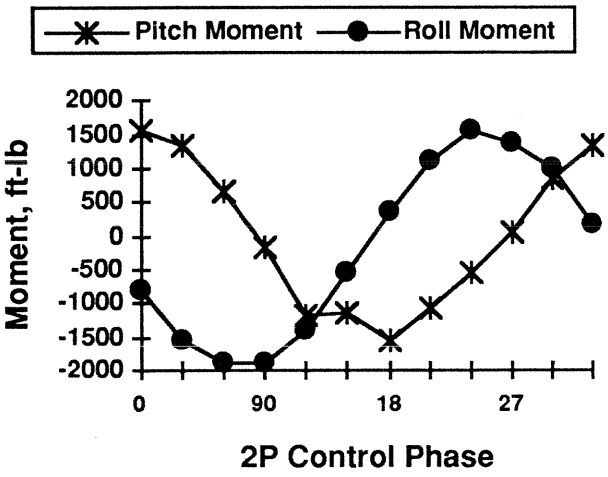

Fig 22. Pitch and roll moment changes at 127 kt, mimimum flapping trim.

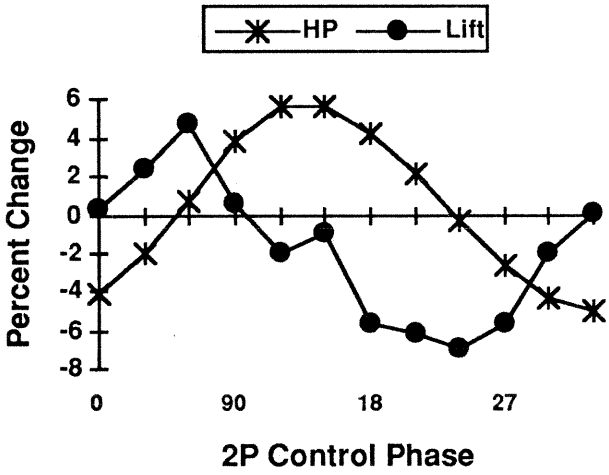

Fig 23. Lift and HP changes at 127 kt, mimimum flapping trim.

change in measured shaft power varied harmonically as the 2P IBC phase angle was varied. This variation was also present in the hub pitch and roll moment, as seen in Fig. 22. From Fig. 23, it would appear that the best 2P control phase angle for power reduction would be 330 deg, where a 5 percent reduction in shaft HP is indicated. However, because of the variations in the rotor trim state, another data set with the rotor trim held constant is required to substantiate this finding. Accounting for the 20 deg phase lag from blade root to blade tip at this input frequency, the 330 deg 2P input would place maximum negative tip pitch angles at about 265 deg and 85 deg rotor azimuth. These phase angles were close to the optimum negative 2P pitch peaks predicted to occur at 90 deg and 270 deg in order to avoid retreating blade stall.

The effect of 2P IBC on performance at high thrust (C_T/s = 0.12) was evaluated for an 85 kt airspeed condition. The change in thrust and rotor power was similar to that seen at 127 kt at 1g thrust. Again, however, another test with the rotor roll moment, pitch moment, and thrust kept invariant with 2P phase angle input is required to assess the true performance gain.

Blade Vortex Interaction Noise

Acoustic data were acquired in an area below the rotor as shown in Fig. 10. For this area, several types of IBC were found to be effective in suppressing BVI noise. IBC inputs tested to reduce BVI noise included single-frequency 2P, 3P, and 6P, as well as pulse, wavelet, and doublet inputs. The best reductions in BVI noise were found using 2P IBC input at phase angles of 60 deg and 270 deg, with 60 deg angle being somewhat better.

Without IBC, Fig. 24A shows a large BVI noise signature riding on top of a lower frequency, blade loading noise component. As shown in the plot, band-pass filtering was used to remove the low frequency loading noise component to more clearly display the BVI noise pressure spikes. At the present time, it is uncertain whether the low frequency noise is only a wind tunnel reverberation effect since it does not appear in flight test data analyzed thus far for the same rotor [Ref. 21].

With ±1.0 deg of 2P IBC at 60 deg input phase angle, Fig. 24B a large decrease in the BVI noise. This amounts to a power reduction of over 7 dB from the baseline case for the BVI frequency bandwidth analyzed. Effectively, 80 percent of the BVI noise signature was removed using 2P IBC. Moreover, the peaks of the low frequency noise component were reduced by half at the same time. Similar reductions in the BVI sound pressure were seen at all microphone locations, but varied somewhat depending on the microphone location.

Although it is obvious that these inputs did something to avoid the blade-vortex interaction, the exact reason the 60 deg and 270 deg 2P inputs reduced the BVI noise is a matter of speculation. The 2P pitch schedules for these two inputs (corrected for tip phase lag) are shown in Fig. 25. Given Fig 25 and considering that the possible mechanisms of BVI reduction include weakening the strength of the tip vortex produced in the second and third rotor plane quadrants, or increasing the vortex-blade miss distance primarily in the first and fourth quadrants [Ref. 22], many scenarios of how the 2P inputs reduced the BVI noise are plausible. It is interesting that the two best inputs are nearly exactly out of phase with each other. Perhaps these inputs change the vortex-blade miss distance, and it doesn't matter much if the distance is increased positive or increased negative.

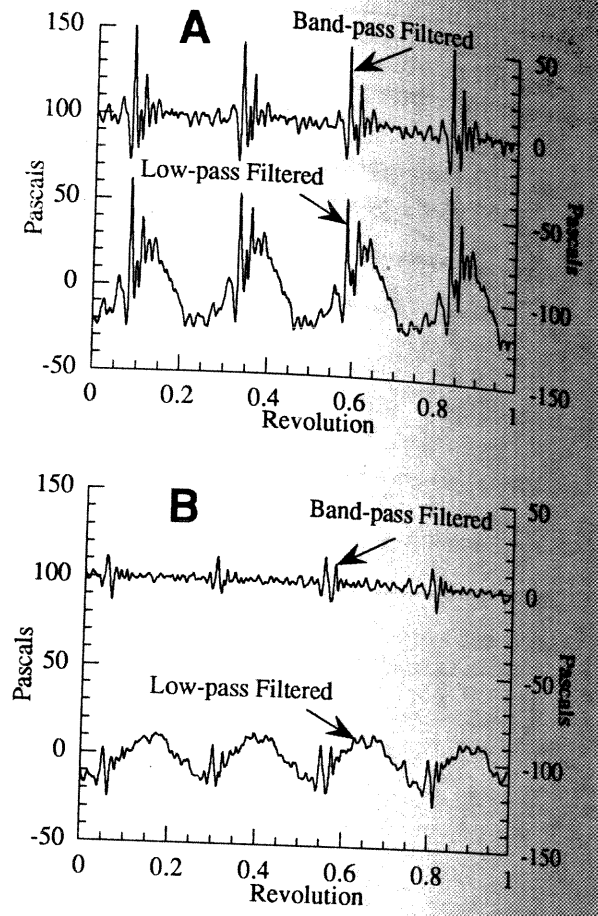

Fig 24. Sound pressure with and without IBC input at 64 kt and minimum flapping trim: A) No IBC and B) ±1 deg 2P IBC at 60 deg phase.

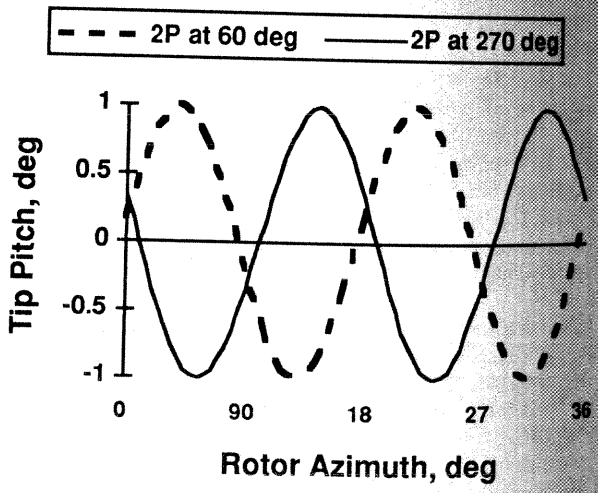

Fig 25. 2P IBC Inputs at phase angles 0 and 60 deg.

An important conclusion to be drawn from the noise reduction achieved with 2P IBC is that a significant BVI noise reduction can be achieved by varying only the phase of the 2P input angle. In Ref. 14 it was shown that feedback control using a single microphone at a representative location on the helicopter fuselage is feasible. However, whereas the controller used in that study formed the measurement state vector from more than a dozen harmonics of the acoustic spectrum, only one may really be needed. This is because only one degree of freedom, the phase of the 2P IBC input, either reduced or increased the BVI power level. Reference 23, presents a more through exposition of the effect of single-frequency and multi-frequency IBC inputs on the BVI noise.

Conclusions

The individual blade control full-scale, wind tunnel test reported herein was a highly successful, cooperative research program conducted by NASA and ZF Luftfahrttechnik under the auspices of the U.S./German MOU in Rotorcraft Aeromechanics. The IBC system, developed by ZF Luftfahrttechnik, was tested on the NASA/Army Rotor Test Apparatus in the Ames 40- by 80-Foot Wind Tunnel. The effect of up to ±1.2 deg of open-loop IBC was studied at two primary forward flight speeds and one condition representative of a descent profile generating relatively high levels of BVI noise.

The IBC functioned well in terms of imparting high-accuracy blade root motions at the desired amplitudes and phases. Good root pitch input accuracy was achieved for IBC amplitudes of ±1.0 mm (±0.34 deg) or more, except for the case of 4P IBC excitation, where an 18 percent amplitude loss occurred.

At the 43 kt condition, single-frequency IBC inputs of 2P - 4P simultaneously suppressed all of the 4P rotor balance forces and moments as much as 50 to 70 percent, depending on the input IBC phase angle. To a lesser extent, the 5P input also achieved a reduction of all hub forces an moments. The 6P IBC inputs were seen to raise vibration at nearly all phase angles.

The effect of IBC on blade and control system loads was studied at the 43 and 127 kt flight conditions. The effect of IBC input was to either raise or lower the blade torsional and chordwise loads depending on the IBC input phase angle. The load on the actuators (pitchlinks) were always higher than without IBC and increased with both increasing amplitude and frequency. The loads on the swashplate produced by the IBC actuator forces limited the IBC input amplitude to ±1.2 deg.

The effect of IBC on rotor performance was uncertain due to variations in the rotor trim state with 2P IBC input. A performance improvement of about 5 percent was measured at the best 2P input phase angle without maintaining trim. Further testing is required to substantiate this finding.

The effect of 2P, 3P, 6P, pulse, wavelet, and doublet IBC inputs were studied to evaluate their effectiveness in reducing BVI noise. The largest reduction of 7 dB was obtained using a 2P input. Reference 23, presents a more detailed discussion of single-frequency and multi-frequency IBC inputs on the BVI noise.

Acknowledgments

The authors wish to thank Mr. Roland Kube (DLR), Mr. Georg Niesl (ECD), Mr. Dietrich Teves (ECD), Mr. Earl Booth (NASA Langley), Dr. Thomas Brooks (NASA Langley), and Dr. William Warmbrodt (NASA Ames) for their helpful comments they made during the IBC testing at Ames. The assistance provided by Mr. Karl-Heinz Bock (ZF Luftfahrttechnik) and Mr. Hans-Jurgen Goette (ZF Luftfahrttechnik) in preparing and operating the IBC system is gratefully acknowledged. Last, but by no means least, many thanks to Mr. Stephen Swanson (Sterling Software) for his help acquiring and analyzing the acoustic data.

References

1) Kretz, M., Auburn, J-N., and Larche, M., "Wind Tunnel Tests of the Dorand DH2011 Jet-Flap Rotor", NASA CR 114693, Volumes 1 and 2, 1973.

2) Lemnios, A.Z., Smith, A.F., "An Analytical Evaluation of the Controllable Twist Rotor Performance and Dynamic Behavior", Kaman Report R-794, 1972.

3) McCloud, J.L., III, and Kretz, M., "Multicyclic Jet-Flap Control for Alleviation of Helicopter Blade Stresses and Fuselage Vibration", NASA SP-352, 1974.

4) Ham, N.D., "Helicopter-Individual-Blade-Control Research at MIT 1977-1985", Vertica, Vol. 11, No. 1/2, 1987.

5) Drees, J. M., and Wernicke, R. K., "An Experimental Investigation of a Second Harmonic Feathering Device on the UH-1A Helicopter," U.S. Army Transportation Research Command, TR-62-109, June 1963.

6) Hammond, C.E., "Wind Tunnel Results Showing Rotor Vibratory Loads Reduction Using Higher Harmonic Blade Pitch", Journal of the American Helicopter Society, Vol. 28, No. 1, Jan. 1983.

7) Wood, E.R., Powers, R.W., Cline, J.H., and Hammond, C.E., "On Developing and Flight Testing

a Higher Harmonic Control System", 39th Annual Forum of the American Helicopter Society, St. Louis, MO, May 1983.

8) Gupta, B.P., Wood, E.R., Logan, A.H., and Cline, J.H., "Recent Higher Harmonic Control Development and OH-6A Flight Testing", 41st Annual Forum of the American Helicopter Society, Ft. Worth, TX, May 1985.

9) Shaw, J., Albion, N., Hanker, E.J., and Teal, R.S., "Higher Harmonic Control: Wind Tunnel Demonstration of Fully Effective Vibratory Hub Force Suppression", 41st Annual Forum of the American Helicopter Society, Fort Worth, TX, May 1985.

10) Straub, F. and Byrns, E., "Application of Higher Harmonic Blade Feathering on the OH-6A Helicopter for Vibration Reduction", NASA CR 4031, 1986.

11) Polychroniadis, M., and Achache, M. "Higher Harmonic Control: Flight Tests of an Experimental System on SA 349 Research Gazelle", 42nd American Helicopter Society Forum, Washington, D.C., June 1986.

12) Miao, W., Kottapalli, S.B.R., and Frye, M. M., "Flight Demonstration of Higher Harmonic Control (HHC) on S-76", 42nd Annual Forum of the American Helicopter Society, Washington, D.C., June 1986.

13) Kube, R., "Evaluation of a Constant Feedback Gain for Closed Loop Higher Harmonic Control", 16th European Rotorcraft Forum, Glasgow, Scotland, September 1990.

14) Kube, R., Achache, M., Niesl, G., and Splettstoesser, W. "A Closed-loop Controller for BVI Noise Reduction by Higher Harmonic Control", 48th Annual Forum of the American Helicopter Society, Washington, D.C., June 1992.

15) Richter, P., Eisbrecher, M.-D, and Kloppel, V., "Design and First Flight Test of Individual Blade Control Actuators", Sixteenth European Rotorcraft Forum, Glasgow, Scotland, September 1990.

16) Teves, D., Kloppel,V., and Richter,P., "Development of Active Control Technologies in the Rotating System, Flight Testing and Theoretical Investigations", Eighteenth European Rotorcraft Forum, Avignon, France, September 1992.

17) Jacklin, S. A., Leyland, J. L., and Blaas, A., "Full-Scale Wind Tunnel Investigation of a Helicopter Individual Blade Control System", AIAA paper No. 93-1361, 34th AIAA/ASME/ASCE Structures, Structural Dynamics, and Materials Conference, La Jolla, CA, April 1993.

18) Richter, P. and Blaas, A, "Full-Scale Wind Tunnel Investigation of an Individual Blade Control System for the BO 105 Hingeless Rotor", Nineteenth European Rotorcraft Forum, Como, Italy, September 1993.

19) Ham, N.D., and Quakenbush, T.R., "A Simple System for Helicopter Individual-Blade-Control and Its Application to Stall Flutter Suppression," Seventh European Rotorcraft Forum, Garmisch-Partenkirchen, Germany, September, 1981.

20) van Aken, J., and Peterson, R.L., "Calibration Results of the NASA Ames Rotor Test Apparatus Steady/Dynamic Rotor Balance", AHS Aeromechanics Specialists Conference on Aerodynamics, Acoustics, and Dynamics, San Francisco, CA, January, 1994.

21) Signor, D. B., Watts, M. E., Hernandez, F. J., and Felker, F. F., "Blade-Vortex Interaction Noise: A Comparison of In-Flight and Small-Scale Mearsurements", AHS Aeromechanics Specialists Conference on Aerodynamics, Acoustics, and Dynamics, San Francisco, CA, January, 1994.

22) Schmitz, F.H. and Yu, Y.H., "Helicopter Impulsive Noise: Theoretical and Experimental Status," NASA TM 84390, November 1983.

23) Swanson, S. M., Jacklin, S. A., Blaas, A., Kube, R., and Niesl, G., "Individual Blade Control Effects on Blade Vortex Interaction Noise," 50th Annual Forum of the American Helicopter Society, Washington, D.C., May 1994.